Geophysical Journal International

Geophys. J. Int. (2011) **184,** 1317–1326 doi: 10.1111/j.1365-246X.2010.04908.x

Triggered seismic activity in the Liquiñe-Ofqui fault zone, southern Chile, during the 2007 Aysen seismic swarm

R. M. Russo,[1] Alejandro Gallego,[1]* Diana Comte,[2] Victor I. Mocanu,[3] Ruth E. Murdie,[4] Cindy Mora[2] and John C. VanDecar[5]

[1]*Department of Geological Sciences, University of Florida, Gainesville, FL, USA. E-mail: rmrusso2010@gmail.com*
[2]*Departamento de Geofisica, Universidad de Chile, Santiago, Chile*
[3]*Department of Geophysics, University of Bucharest, Bucharest, Romania*
[4]*Gold Fields Australia, St. Ives Gold Mine, P.O. Box* 359*, Kambalda, WA* 6442*, Australia*
[5]*DTM, Carnegie Institute of Washington,* 2541 *Broad Branch Road, Washington, DC* 20015*, USA*

Accepted 2010 November 29. Received 2010 October 12; in original form 2010 January 18

SUMMARY

We relocated the six large-magnitude ($5.2 < M_w < 6.2$) earthquakes of the destructive, tsunamigenic Aysen seismic swarm, which occurred from 2007 January–October in Patagonian Chile. We used *P* and *SH* arrival times from near-source stations of a temporary seismic network fortuitously deployed in the area when the swarm began, and also traveltimes to stations of the permanent global networks, to locate the 2007 January 23, M_w 5.2 earthquake, the first of the six large magnitude events. This earthquake's hypocentre lies at shallow depth (<10 km) on the eastern strand of a major intraarc shear zone, the dextral Liquiñe-Ofqui fault zone. Using the hypocentre of the January 23 earthquake as a fixed location, we relocated the five other large magnitude Aysen earthquakes by joint hypocentral determination. Four of these five events also occurred at shallow depth on the eastern strand Liquiñe-Ofqui fault, whereas the 2007 April 2, earthquake occurred some 45 km to the west on the Aysen fault, a strike-slip duplex fault that segments the area between the eastern and western Liquiñe-Ofqui fault strands. The five earthquakes on the Liquiñe-Ofqui fault were all produced by dextral slip on ∼N–S nodal planes approximately parallel to the mapped trace of the fault. The April 2 earthquake resulted from normal slip on the Aysen fault. Modelling of Coulomb stress changes on the nodal planes of the April 2 earthquake shows that the cumulative slip on the Liquiñe-Ofqui fault strand could have triggered the April 2 earthquake. Similarly, the April 2 earthquake may have triggered the M_w 6.2 April 21 earthquake, which caused mass wasting into Aysen Fjord, generating a destructive tsunami. The system of channels and fjords in the study region is a major shipping route around South America, and therefore careful evaluation of the seismic hazard is warranted.

Key words: Tsunamis; Earthquake interaction, forecasting and prediction; Seismicity and tectonics; Transform faults; Continental margins: convergent; Neotectonics.

1 INTRODUCTION: THE LIQUIÑE-OFQUI FAULT ZONE

The Liquiñe-Ofqui fault is a dextral intraarc strike-slip fault zone consisting of two major strands (Cembrano *et al.* 1996, 2002; Rosenau *et al.* 2006; Wang *et al.* 2007; Lange *et al.* 2008) extending north from the Nazca–Antarctica–South America triple junction in Chilean Patagonia (Fig. 1). GPS site velocities in the vicinity of the Liquiñe-Ofqui fault zone (LOFZ) clearly show that the fault forms the eastern boundary of a wide forearc sliver, currently translating northward with respect to South America (Fig. 1; Wang *et al.* 2007). Field studies of the fault zone reveal both ductile and brittle kinematic indicators in the Cenozoic intrusive North Patagonian Batholith and metamorphic wall rocks cut by the fault (Cembrano *et al.* 1996, 2002; Arancibia *et al.* 1999). These displacement features are consistent with late Cenozoic dextral slip on the fault, although older, mylonitic deformation associated with the fault zone may indicate that the original sense of motion was left-lateral and took place at deeper levels in the crust. Paleomagnetic data of blocks in the LOFZ are consistent with vertical axis block rotations within the fault system (Cembrano *et al.* 1992; Beck *et al.* 1993; Rojas *et al.* 1994). The fault zone is believed to have formed via partitioning of deformation in the overriding South America forearc due

*Now at: Department of Geology and Geophysics, School of Ocean and Earth Science and Technology, University of Hawai'i at Mānoa, POST Building, Suite 701, 1680 East-West Road, Honolulu, HI 96822, USA.

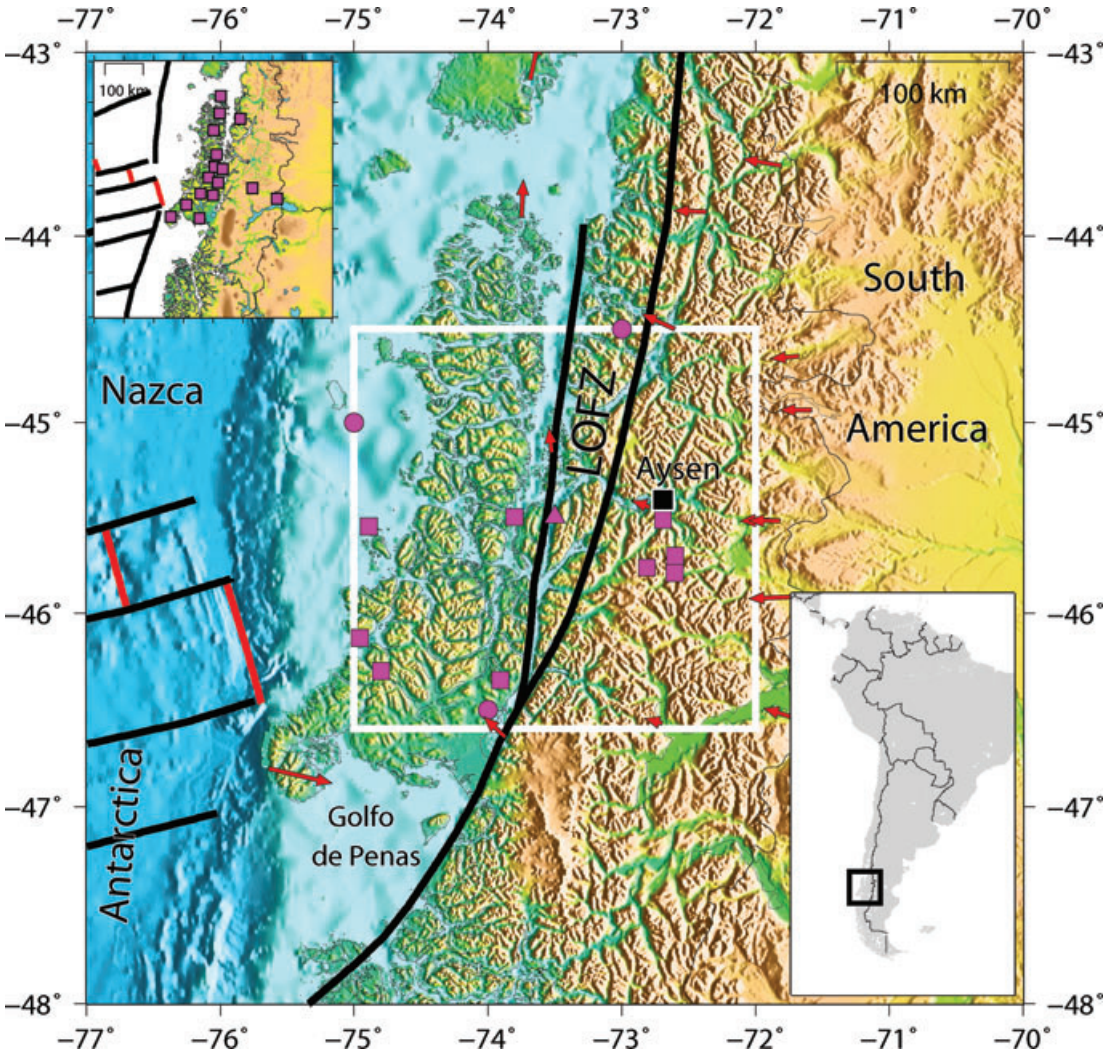

Figure 1. Topography and bathymetry of study region. LOFZ is the Liquiñe-Ofqui fault zone, which bifurcates to form eastern and western strands. Red arrows are GPS site velocities of Wang *et al.* (2007). Purple symbols are epicentres of earthquakes prior to 2007; depths: circles—0.25 km; squares—25 to 50 km; triangle—50 to 75 km. Black square: city of Aysen location. Inset, upper left-hand side: Map of CRSP stations in operation during January–February 2007, when the Aysen earthquakes began. White box marks area of Fig. 4.

to oblique subduction of the Nazca Plate (Pardo-Casas & Molnar 1987; Rosenau *et al.* 2006; Wang *et al.* 2007; Lange *et al.* 2008) and the changes in its sense of motion may reflect variability in this obliquity (Cembrano *et al.* 1996).

The region between the two strands of the LOFZ north of ∼46.5°S is segmented by four NE–SE striking normal faults (Fig. 2) forming a strike-slip duplex, or horsetail splay, within the strike-slip fault system (Cembrano *et al.* 1996; Arancibia *et al.* 1999). From north to south, the Puyuguapi, Aysen, Quitralco and Francisco faults cut the Chilean coastline forming deep NE-trending fjords. The Aysen splay fault underlies the western, NE–SW trending portion of Aysen Fjord and apparently extends at least to the northeastern coast of Isla Traiguén (Fig. 2). Details of the intersection of this fault and the western LOFZ strand are poorly known because its western trace is submarine in the channel system. We show below that this fault is active and participated in the 2007 earthquake swarm.

Seismic activity along the LOFZ has been poorly studied to date, largely because teleseismic events clearly related to the fault have been few (Fig. 1) and local or regional seismicity associated with the fault has gone unrecorded because of a lack of seismic stations in the vicinity of the fault. Cifuentes (1989) reported several modest, shallow, shocks with dextral strike-slip mechanisms that may have occurred on the Liquiñe-Ofqui, but no ground breaks were observed and the teleseismic locations are not sufficiently accurate to be definitive. Murdie *et al.* (1993) operated a seismic network in the study region for several months during 1992 but recorded no earthquakes that could be attributed to the LOFZ. Haberland *et al.* (2006) and Lange *et al.* (2007, 2008) report seismic activity on the northernmost portion of the LOFZ, east of Chile, some 200 km north of our study area. Thus, prior to 2007, seismic activity on the southern portion of the LOFZ was an open question. Discussions of seismic hazard in this region centred on the possibility of a repeat of the great 1960 Chile earthquake.

2 THE 2007 AYSEN EARTHQUAKES

The Aysen earthquakes began on the afternoon (UTC) of 2007 January 10, with a single small shock ($M_L < 3$) at shallow depth beneath Aysen Fjord. More events occurred in the same location

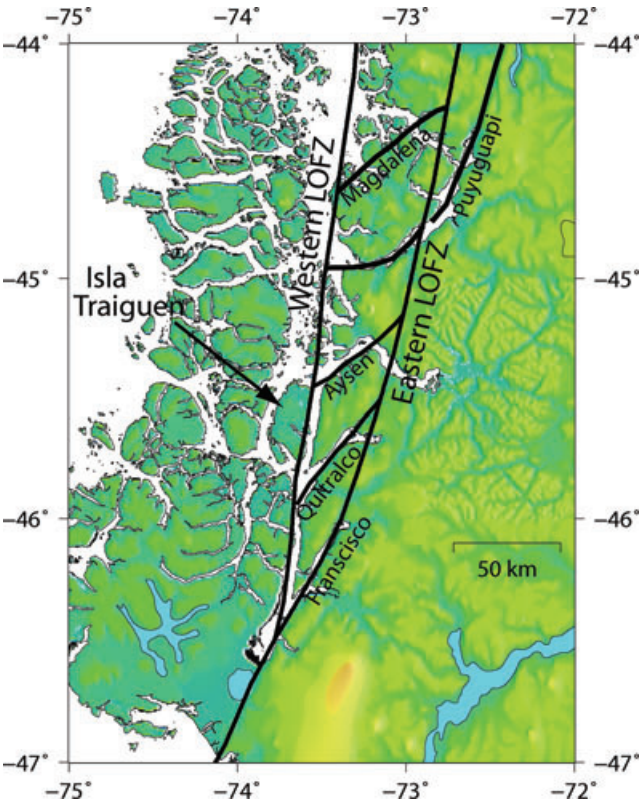

Figure 2. Horsetail splays of the LOFZ fault zone, modified from Arancibia *et al.* (1999).

on January 14, 18 and 19, six earthquakes on January 21 and finally some 80 events, including an M_w 5.3 shock at 20:40:11.3 (Table 1), on January 23. Over the course of the next 10 months, thousands of earthquakes occurred beneath the Fjord, ultimately including six events with magnitude ≥5.2 (Table 1). Mora *et al.* (2010) have shown, by locating aftershocks of the January 23 earthquake recorded at stations of the temporary Chile Ridge Subduction Project (CRSP), that the Aysen earthquakes occurred on the eastern strand of the LOFZ where it crosses Aysen Fjord (Fig. 3). These events define a steeply west-dipping plane striking NNE and bottom out at 8–9 km depth. Focal mechanisms of the low-magnitude swarm earthquakes recorded on the CRSP stations show predominantly dextral strike-slip on ∼N–S striking nodal planes, consistent with geologic and geodetic studies of the LOFZ, as outlined above. The fortuitous deployment of the CRSP seismic network in the Aysen swarm region allowed us to examine the six larger magnitude Aysen earthquakes in some detail.

3 EARTHQUAKE RELOCATIONS

The six larger magnitude Aysen swarm earthquakes can only be understood and the precise relationship between them can only be addressed, if the hypocentres of the events are well known. The CRSP temporary seismic deployment was actually being demobilized when the swarm began in 2007 January and was entirely dismantled by 2007 February 9, and thus only the first three of the six earthquakes studied were recorded in any way by the near-source network (Table 1). However, all six events were well recorded on stations of the various global seismic networks, and arrival time data for all six are available from the International Seismological Centre (ISC). We therefore adopted a two-step relocation procedure: First, we picked *P*- and *S*-wave arrival times for the 2007 January 23, January 28 and February 3, earthquakes on vertical (*P*) and transverse horizontal (*SH*) seismograms of the operating CRSP network stations, assuming the teleseismic hypocentres reported by the USGS were valid. Next, we added these times to those tabulated by the ISC for the three earthquakes and determined new locations for the events using both the local/regional CRSP arrival times and those from the global network stations. The locations were determined using a generalized linear inverse routine that minimizes differences between the observed event-station traveltimes and those predicted for a trial location based on the IASP91 radial earth model (Kennett *et al.* 1995). Traveltime residuals were then recalculated based on the new location and the solutions iterated to convergence (Wysession *et al.* 1991; Russo *et al.* 1992). The relocated hypocentre of the 2007 January 23, earthquake lies on the eastern strand of the LOFZ (Fig. 2) at very shallow depth (fixed at 10 km, but very likely shallower; comparison of rms residuals for varying estimates of the fixed hypocentral depths of the events shows that minimum residuals occur for depths shallower than 10 km for five of the six events and shallower than 12 km for the remaining earthquake; see Table 1). The rms residual of observed minus calculated arrival times was 3.40 s for 78 stations spanning a distance range from 0.45° to 96.07°Δ. Since this event's hypocentre was based on the most traveltime picks from the near-source CRSP network, we adopted it as the master event hypocentre for the second part of the relocation procedure. Note that the relocations we present here are distinct from the locations determined by Mora *et al.* (2010), who located only the January 23 event and 132 of its small-magnitude fore- and aftershocks, all of which occurred during 2007 January; none of the five other events relocated in our study were treated by Mora *et al.* (2010).

The six study earthquakes were recorded by nearly all the same stations from the global seismic networks, and thus, given the master event location determined as above, are amenable to relative location schemes such as joint hypocentral determination (JHD, Douglas 1967; Dewey 1972; Marshall & Russo 2005). The JHD relocation scheme uses observed traveltime differences for distinct events recorded at the same stations to derive a relative location

Table 1. Earthquake parameters.

Date	Origin time	South latitude (°)	West longitude (°)	Depth range (km)	M_w	M_o (dyne-cm)	Strike (°)	Dip (°)	Slip (°)
2007 January 23	20:40:11.3	45.4067	73.0996	1–10	5.3	1.29×10^{24}	354	89	–179
2007 January 28	02:53:14.0	45.4029	73.1198	1–12	5.2	7.7×10^{23}	14	89	166
2007 February 3	09:00:13.5	45.3601	73.1709	1–10	5.3	1.25×10^{24}	182	84	–174
2007 February 23	19:55:41.9	45.3468	72.9873	1–10	5.7	4.12×10^{24}	181	79	–160
2007 April 2	02:49:31.1	45.4472	73.6762	1–10	6.1	2.07×10^{25}	53	43	–86
2007 April 21	17:53:38.6	45.3293	73.2073	1–10	6.2	2.84×10^{25}	354	88	176

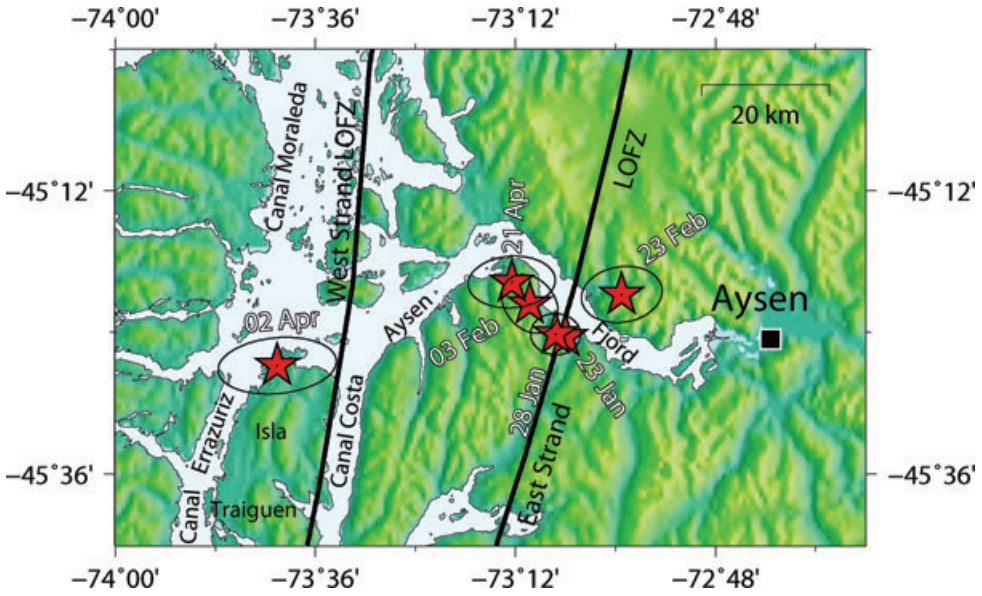

Figure 3. JHD locations of six Aysen large magnitude events. Stars mark epicentre, ellipses are 90 per cent confidence limit.

offset from a designated master event. The earthquakes included in the relocation procedure must have occurred near enough to each other that no significant differences in Earth structure are expected for the source-station travel paths. Using the JHD scheme, we find that four of the earthquakes relocate to very shallow hypocentres along Aysen Fjord on or near the eastern strand of the LOFZ (Figs 2 and 3, Table 1) and within ∼10 km of the master event hypocentre. Hypocentres of the true aftershocks of the 2007 January 23, earthquakes, located by Mora *et al.* (2010), also lie on the eastern strand of the LOFZ clustered about our master event location.

The 2007 April 2, hypocentre, in contrast, lies at shallow depth some 45 km west of the other events near the north coast of Isla Traiguén (Figs 2 and 3). This event's focal mechanism represents almost pure dip-slip normal faulting on one of two planes striking NE–SW and dipping ∼45 either NW or SE (Fig. 4). Given its location and focal mechanism, the April 2 event likely occurred on the Aysen fault (Fig. 2) near its junction with the western LOFZ in the vicinity of the north coast of Isla Traiguén.

4 EARTHQUAKE TRIGGERING AND COULOMB FAILURE MODELLING

4.1 2007 April 2, normal faulting earthquake

The 2007 April 2, earthquake is unlike the other Aysen earthquakes in that its focal mechanism clearly indicates normal faulting on nodal planes striking NE–SW, dipping 53°SE and 47°NW (Global Centroid Moment Tensor (CMT) focal mechanisms), whereas the five other study earthquakes have clear right-lateral strike-slip (RLSS) mechanisms on ∼N–S planes approximately parallel to the local strike of the eastern LOFZ strand (Fig. 3). Given the apparently low rate of seismicity in the study region prior to the Aysen earthquakes in 2007, the modest spatial separation between the April 2 and other events, and the fact that the April 2 event occurred during the swarm of Aysen RLSS earthquakes, it seems reasonable to ask whether or not the April 2 event was in some way triggered by the slip events on the eastern LOFZ. The near-simultaneity of the events (all within ∼4 months) and the 45 km separation between the swarm and April 2 hypocentre point to interaction of static stress changes between the two source regions, as opposed to time-dependent interactions mediated by propagation of viscous deformation (e.g. Pollitz & Sacks 1992, 1997; Toda & Stein 2003).

We examine whether or not the slip on the eastern LOFZ during the four swarm earthquakes that occurred prior to the April 2 earthquake could have induced static stress changes, which triggered the April 2 normal faulting on the Aysen strike-slip duplex normal fault. Such interactions have been observed for earthquakes in California, Japan, Anatolia and Taiwan (King *et al.* 1994; Harris 1998; Stein 1999, 2003; Toda & Stein 2003; Lin & Stein 2004; Ma *et al.* 2005). The Coulomb stress change on a fault close to failure due to slip on another fault in the environs is modelled as

$$\Delta\mathrm{CFF} = \Delta\tau + \mu\Delta\mathrm{s},$$

where $\Delta\tau$ and $\Delta\sigma$ are the shear stress and normal stress changes on the receiver fault, respectively and μ is the effective coefficient of friction on the receiver fault, modified to take into account pore fluid pressure. $\Delta\tau$ is positive in the slip direction and $\Delta\sigma$ is positive when the fault is unclamped. Stress changes due to slip on one fault thus accelerate failure on neighbouring faults when both the shear stress and unclamping normal stress on the receiver faults are increased (King *et al.* 1994; Lin & Stein 2004; Toda *et al.* 2005). In our case, the geometry of both the master fault (RLSS on the eastern strand of the LOFZ) and the receiver fault are reasonably well known (Table 1), so we can calculate the stress changes on the April 2 earthquake fault directly.

We used the Coulomb 3 program (Lin & Stein 2004; Toda *et al.* 2005) to calculate ΔCFF, based on the input parameters shown in Table 2. The model rheology is elastic with faults embedded in a half-space, their positions scaled according to the earthquake relocations described above. Fault orientations derive from the event CMT focal mechanisms (Table 1; Ekstrom *et al.* 2006). In a linear elastic medium, repeated slip on a given fault, such as that produced by the four very similar strike-slip study earthquakes that preceded the April 2 earthquake (Fig. 3), can be modelled as a single event with equivalent summed magnitude and slip (King *et al.* 1994). The magnitudes of the four earthquakes were modest ($M_w < 5.7$) and their summed scalar moment was only 7.43×10^{24} dyne-cm, so

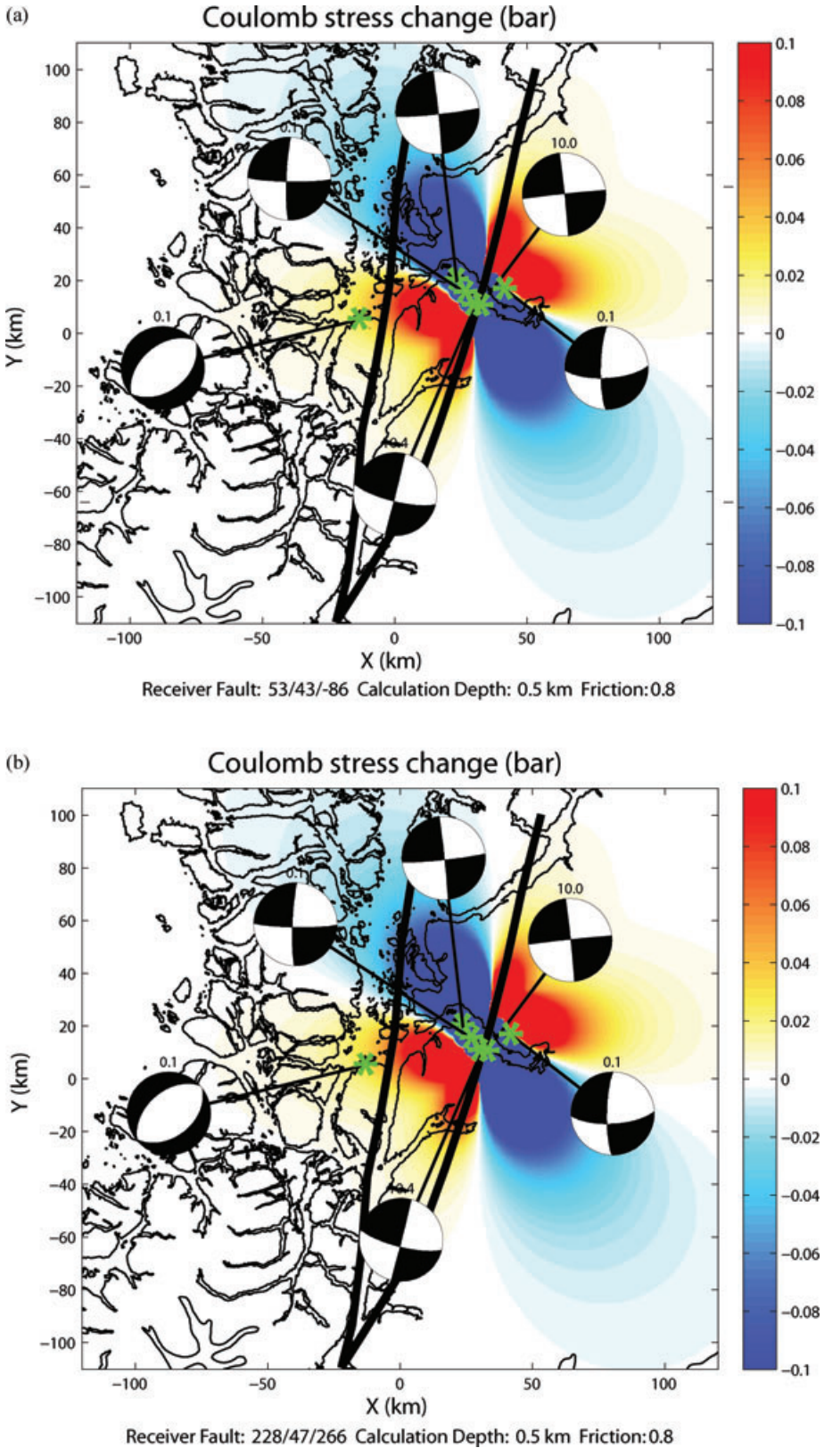

Figure 4. (a) Coulomb stress change due to cumulative slip of four events preceding April 2 earthquake on the eastern strand of the LOFZ. Nodal plane for the April 2 event dips SE. CMT focal mechanisms from Ekstrom *et al.* (2006). April 2 hypocentre lies in a lobe of increased Coulomb failure stress (warm colours). (b) Coulomb stress change due to cumulative slip of four events preceding April 2 earthquake on the eastern strand of the LOFZ. Nodal plane for the April 2 event dips NW. CMT focal mechanisms from Ekstrom *et al.* (2006). April 2 hypocentre lies in a lobe of increased Coulomb failure stress (warm colours).

Table 2. Modelling parameters.

Poisson's ratio	0.25
Young's modulus	8.0×10^5 bar
Fault slip	0.3 m
Fault length	22 km
Fault width (downdip)	4.4 km
Calculation depth	0.5 km

we estimated the equivalent slip based on observed magnitude–slip relationships (Stein & Wysession 2003), obtaining a summed slip of ∼0.3 m. The earthquake magnitudes were too low to warrant modelling of variable slip on the fault plane, so we adopted the summed slip value as an average for the entire ruptured region. The fault dimensions were similarly estimated, yielding a nominal area of 100 km^2.

Although there is no ambiguity in the fault plane for the four strike-slip study events, which occurred on the ∼N–S trending eastern strand of the LOFZ (Mora *et al.* 2010), which of the two possible receiver fault nodal planes slipped during the April 2 event is not known. When the effective friction, μ, on the receiver fault(s) is non-zero, the Coulomb stress change on the two possible nodal planes differs (Ma *et al.* 2005). The effective coefficient of friction on faults is likely to be low, even zero, if the faults are zones of major displacement or high pore pressure; however, young faults with small throw are more likely to be rough, with high coefficients of friction ∼0.8 (Lin & Stein 2004). It is difficult to argue that the fault that slipped to produce the April 2 earthquake is a major displacement surface, given the paucity of observed seismicity in the study region. Pore pressures in the fault are also likely to be low since the fault is a shallow normal fault with moderate dip (∼45°). Note also that evidence of neotectonic activity, including normal faulted grabens bounded by faults oriented parallel to the shallow slip surface of the April 2 event, were observed by us on the northern part of Isla Traiguén (Figs 2 and 5) near the April 2 epicentre, so the April 2 fault could very well be young and rough with high coefficient of friction. Given the uncertainties, we calculated ΔCFF for both possible April 2 nodal planes and for μ values of 0.0, 0.4 and 0.8.

We find a similar pattern of Coulomb stress change due to the slip on the eastern strand of the LOFZ for both potential April 2 nodal planes and for all three modelled fault friction states (Fig. 4): the relocated hypocentre of the April 2 event clearly lies within a lobe of increased ΔCFF. The magnitude of the Coulomb stress change increases with increasing μ, but is modest for all three friction values, ranging from around 0.05 bar for $\mu = 0.8$ to ∼0.02 bar for $\mu = 0.0$. For the reasons mentioned above, the coefficient of friction is likely to be on the high end of the modelled range, so we prefer the Coulomb stress change results for $\mu = 0.8$, shown in Fig. 4.

4.2 2007 April 21, LOFZ strike-slip earthquake

The April 2 earthquake was followed on April 21 by a magnitude M_w 6.2 earthquake apparently on the eastern LOFZ in the vicinity of the previous larger magnitude RLSS swarm events (Fig. 3). Shaking from the April 21 event caused significant damage in the city of Aysen and surroundings and also caused a series of landslides along the steep-sided Aysen Canal that dumped debris into the navigation channel. The resulting 1–2 m tsunami, channelized in the Fjord, resulted in serious damage to vessels and infrastructure of the Port and killed two.

Sequences of earthquake triggering in near temporal proximity are known from other localities (e.g. King *et al.* 1994; Stein 2003), so we assessed the possibility that, having been triggered by slip on the LOFZ, the April 2 Aysen Fault earthquake might have triggered the April 21 shock in the vicinity of the Aysen swarm events, proper. We note that the two April earthquakes, at $M_w > 6$, were the largest shocks of the entire 2007 sequence, and thus the most likely to change stresses on neighbouring faults. Coulomb stress changes due to 1 m mean slip on either of the two April 2 nodal planes, assuming a fault area of some 270 km^2, as appropriate for the event's magnitude (Stein & Wysession 2003), are shown in Fig. 6.

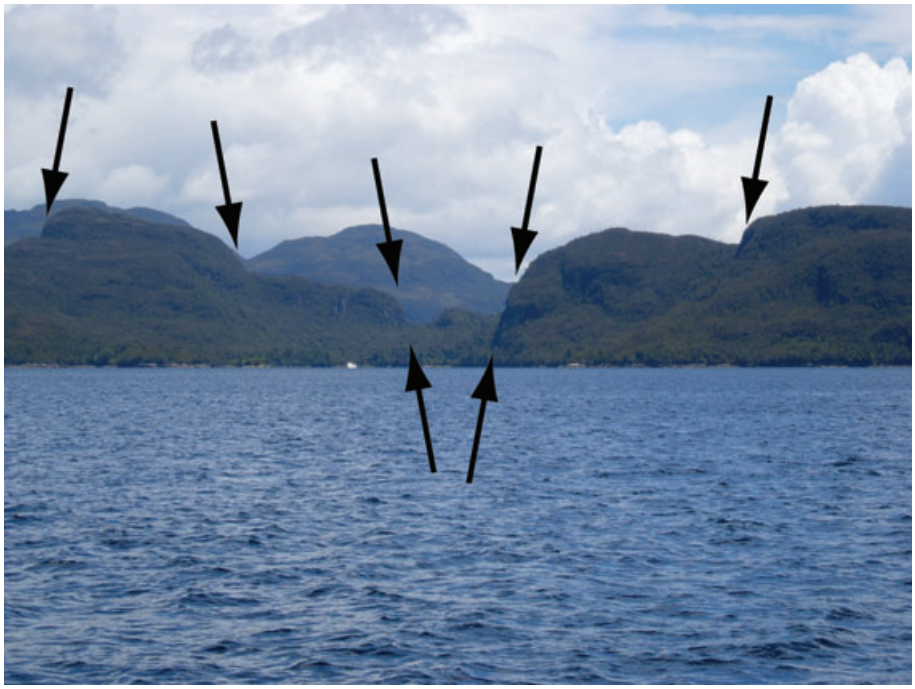

Figure 5. Normal faulting on northeastern coast of Isla Traiguén. Central graben scarps appear to be recent, postglaciation. Photo from NE looking SW.

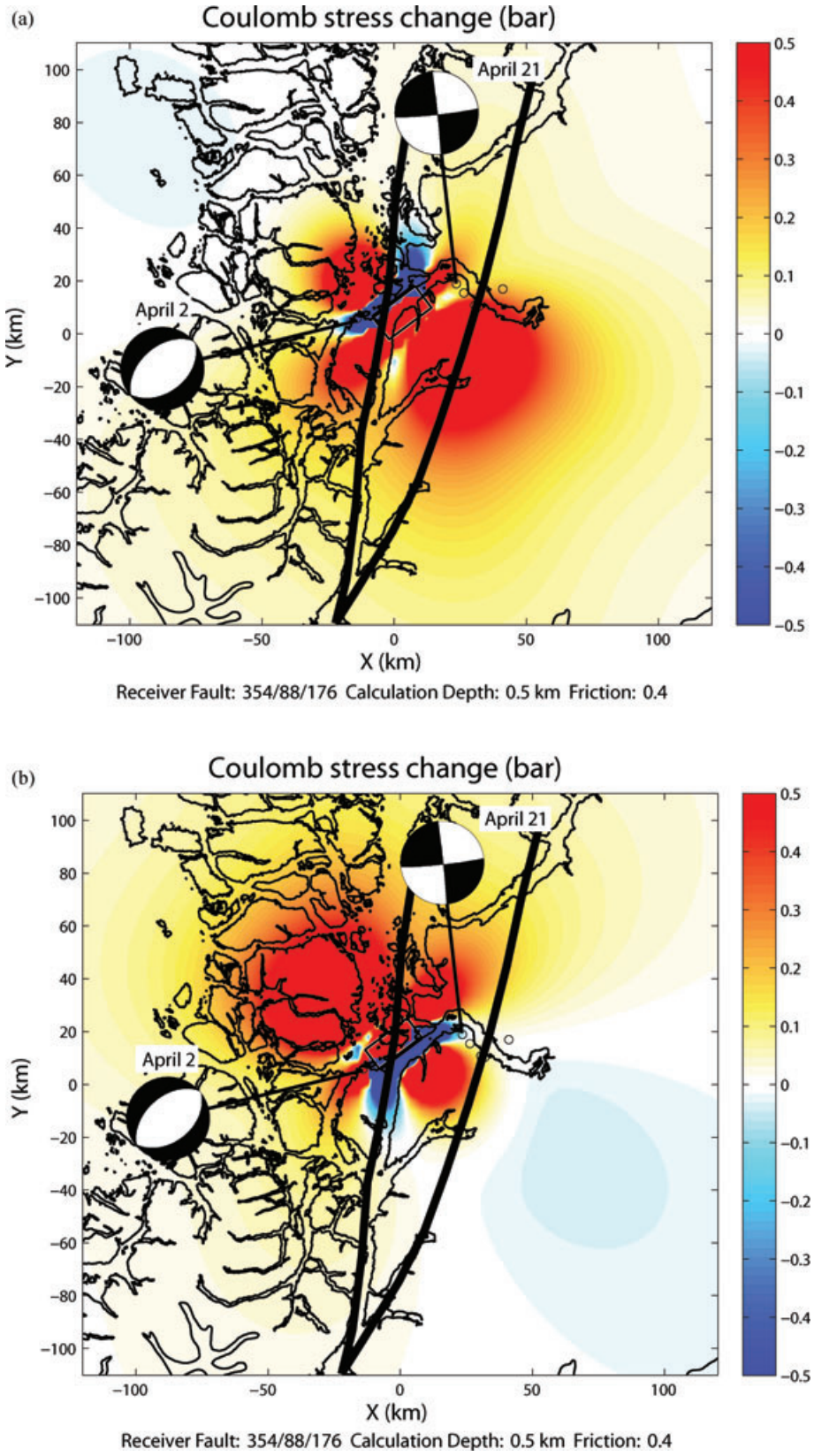

Figure 6. (a) Coulomb stress changes due to slip on SE-dipping nodal plane of April 2 earthquake on the Aysen fault. CMT focal mechanisms from Ekstrom *et al.* (2006). Hypocentre of the RLSS April 21 earthquake lies on the margin of a lobe of increased Coulomb failure stress (warm colours). (b) Coulomb stress changes due to slip on NW-dipping nodal plane of April 2 earthquake on the Aysen fault. CMT focal mechanisms from Ekstrom *et al.* (2006). Hypocentre of the RLSS April 21 earthquake lies on the margin of a lobe of decreased Coulomb failure stress (cool colours).

In these calculations, the ∼N-striking nodal plane of the focal CMT mechanism of the April 21 earthquakes (Ekstrom *et al.* 2006) was taken as the orientation of the receiver fault. Because the LOFZ is considered to be a long-lived fault (e.g. Cembrano *et al.* 1996), we reduced the coefficient of friction on the fault to 0.4; other model parameters were as described above.

Coulomb stress changes in the vicinity of the April 21 hypocentre differ depending on whether or not the plane that ruptured during the April 2 earthquake dips NW or SE: A southeasterly dip places the April 21 JHD hypocentre and the region of the early Aysen swarm earthquakes (Mora *et al.* 2010), in a lobe of increased Coulomb stress and thus could have accelerated slip (Fig. 6a). However, the lobe of increased Coulomb stress SE of the April 2 rupture is much smaller for a northwesterly dipping Aysen fault and if the April 21 JHD hypocentre actually lies at the centre of its 90 per cent confidence ellipse (as shown in Fig. 6b; see Fig. 3 for the ellipse), the calculated Coulomb stress change there is negative, indicating a tendency to suppress slip on faults in the orientation of the April 21 earthquake.

5 DISCUSSION

5.1 Earthquake relocations

The hypocentre of the January 23 earthquake, the first of the six larger magnitude shocks we studied, falls precisely on the mapped trace of the eastern strand of the LOFZ (Fig. 3). We consider this event to be the best located of the earthquakes we studied, given that its hypocentral location is based on the most near-source data from the CRSP temporary network. The increasing areas of the subsequent events' 90 per cent confidence ellipses reflect the relative degradation of the locations as the CRSP network was dismantled and the number of near-source stations decreased. Note also that the major axes of the error ellipses are longer in longitude than latitude, generally, reflecting the fact that very few recording stations within range of direct *P* waves with lower mantle turning points lie to the west of the study region.

The four JHD South Pacific stations that do lie in the western quadrant are all essentially along the same azimuth from the Aysen source region. Station corrections for all four were positive and significantly larger than any other station corrections calculated in the final, converged joint solution. The rms of station corrections to these western stations, PPT, TVO, PAE and VAH, was 5.9 s, whereas that for all other stations (45) was 1.8 s. These western azimuth station corrections thus appear to be systematically overestimated. This overpartitioning of traveltime residuals into station corrections affects all five of the JHD hypocentres equally, given the nature of the output: hypocentres relative to the master event location. However, assigning a portion of the traveltime residuals to station corrections does figure in the estimates of the event uncertainty ellipses, and the geometry of this particular group of western stations largely controls the east–west extent of the event uncertainty ellipses. A greater fraction of that uncertainty has been partitioned into these station corrections, so we consider the east–west semi-major axes of the ellipses to be underestimates. Experiments using different combinations of 45 stations in the JHD routine suggest that the underestimate of the 90 per cent confidence limit is ∼30 per cent. In contrast, the distribution of recording stations north and south of the study area is such that event locations and uncertainties are not changed significantly when stations are swapped in or out of the JHD routine. It is important to note that in none of these experiments did the hypocentre of the April 2 earthquake merge into the group of remaining hypocentres to the east—this event's epicentre is distinct and relocates to an area around the north coast of Isla Traiguén for the groups of input stations we tested.

Confidence ellipses longer in east–west extent for the four more eastern events intersect the mapped LOFZ in the vicinity of Aysen Fjord. Thus, as above, our preferred interpretation is that all five of these dextral strike-slip events occurred in same area along the LOFZ. However, the April 2 event remains distinct in its location and by its normal faulting mechanism.

5.2 Coulomb stress modelling

The Coulomb stress change modelling results clearly indicate that the April 2 normal faulting earthquake on the Aysen fault could have been triggered by the cumulative slip of the four larger-magnitude Aysen earthquakes that preceded it. The low magnitude of ΔCFF we calculate, even for the highest value of fault friction we consider, is consistent with imminent slip on the April 2 earthquake fault plane—whichever nodal plane actually slipped—prior to the Aysen swarm events: The April 2 fault must have been very close to failure before the strike-slip events occurred on the eastern strand of the LOFZ.

Whether or not the April 2 event triggered the April 21 earthquake is less clear. If the Aysen Fault dips to the SE, then the best epicentre of the April 21 earthquake lies in a lobe of increased Coulomb stress of magnitude ∼0.3 bars. If the April 21 M_w 6.2 earthquake did in fact occur on the LOFZ near the hypocentre of the January 23 master event, then the Coulomb stress change on the Liquiñe-Ofqui was increased by around 0.5 bar by the slip on the Aysen Fault on April 2. If, on the other hand, the Aysen Fault dips to the NW, the best epicentre of the April 21 earthquake lies in a lobe of modestly decreased Coulomb stress (Fig. 6b). Adopting a location for the April 21 earthquake along the LOFZ near that of the January 23 master event again places the rupture in a lobe of increased Coulomb stress (by ∼0.2 bar), also allowing the possibility of triggering of the April 21 earthquake. Horsetail splay faults typically dip in the direction of slip along the master strike-slip fault, which for the LOFZ would imply a northwest dip for the Aysen Fault. Thus, if the April 2 event triggered slip on the LOFZ on April 21, the most acceptable interpretation would appear to be that slip occurred on a NW-dipping Aysen Fault and the April 21 slip occurred on the eastern strand of the LOFZ and not off the fault some 10 km to the west, as the best JHD epicentre would indicate.

We note that the study area was almost completely devoid of teleseismically located seismicity throughout the entire period of instrumental seismological recording prior to the 2007 earthquakes, and thus the near simultaneity of the April 2 and the eastern LOFZ strike-slip earthquakes is suggestive. The April 21 rupture, following four other earthquakes of significant magnitude and thousands of smaller magnitude shocks, indicates that accumulated stress on the LOFZ was not significantly relieved by the earlier earthquakes. Maintenance of the LOFZ near failure at least until the April 21 earthquake would be consistent with triggering or hastening of slip on the LOFZ by the modest Coulomb stress changes caused by the April 2 earthquake. An increasing body of evidence indicates that earthquakes and other fault slip phenomena can be triggered by very small stress changes (e.g. Freed 2005; Schwartz & Rakosky 2007). However, the behaviour of the LOFZ appears to be unusual in comparison with other continental strike-slip faults like the San Andreas or North Anatolian faults: accumulated stress appears to

have been released over a period of months, but as seismogenic slip, not creep; the fault appears to have remained near failure for some 4 months at least and stress was not released in a cascading rupture yielding a distinct larger magnitude earthquake, but rather was relieved by five M_w 5.2–6.2 earthquakes.

5.3 Seismic hazard

The Aysen seismic swarm culminated with the M_w 6.2 2007 April 21, strike-slip earthquake on the eastern strand of the LOFZ. This damaging earthquake caused a number of landslides in the source region, including notable slope failures along the Aysen Fjord that resulted in a 1–2 m high tsunami in the Fjord. The wave was channelized and propagated to the harbour of Aysen, damaging infrastructure and vessels and resulting in two deaths. The prospect that even modest magnitude earthquakes in the Aysen region can trigger secondary seismicity like the April 2 earthquake, and also generate tsunamis via landslides into the canal system is sobering. The channels of the study area, particularly Canal Moraleda, Canal Costa, Canal Errazuriz and Aysen Fjord (Fig. 3) are seaways facilitating transport of much of the ocean-borne traffic around South America. The potential for a catastrophic tsunami generated by triggered seismicity should be evaluated carefully in light of the results of our study.

6 CONCLUSIONS

We relocated the six larger magnitude ($5.2 < M_w < 6.2$) earthquakes of the January–October 2007 Aysen seismic swarm, using a combination of traveltimes from the temporary CRSP seismic network and arrival time data collected and made available by the ISC. To take advantage of well-recorded *P* and *SH* arrivals at the CRSP stations, the relocations proceeded in two steps. First, we located the January 23 and 28 earthquakes and the February 3 events using all available traveltime data in a generalized linear inversion scheme. Subsequently, we used the resulting location of the January 23 earthquake as a fixed hypocentre in a master event JHD scheme to find locations of the other five earthquakes relative to the January 23 event. Five of the six large magnitude earthquakes of the Aysen swarm occurred at shallow depths (<10 km) on the eastern strand of the LOFZ and were caused by dextral slip on that fault. The 2007 April 2, Aysen earthquake, in contrast, occurred at shallow depth on the Aysen fault, one of four faults that segment the LOFZ into a strike-slip duplex, or horsetail splay, in the study area. Slip during the April 2 earthquake was nearly pure dip-slip normal faulting along one of two nodal planes striking NE–SE and dipping $\sim 45^\circ$ either SE or NW.

We calculated Coulomb stress change on the nodal planes of the April 2 earthquake due to the cumulative slip of the four eastern LOFZ earthquakes that preceded it, to determine if the April 2 earthquake could have been triggered by the slip on the other fault. We find that Coulomb failure stress was increased by a modest amount (0.02–0.05 bar) on either of the two possible April 2 nodal planes. The relatively low value of the Coulomb stress increase probably indicates that the Aysen fault was very close to failure prior to the Aysen swarm earthquakes.

Coulomb stress changes on the LOFZ in the vicinity of the dextral April 21 earthquake, due to the slip on the Aysen Fault on April 2, however, are more equivocal. If the April 2 rupture occurred on a SE-dipping Aysen Fault, the April 21 event could have been triggered by a modest increase in Coulomb stress. If the Aysen Fault dips to the NW, the best hypocentre of the April 21 earthquake lies in a lobe of modestly lowered Coulomb stress.

ACKNOWLEDGMENTS

Many thanks to Liz Screaton for setting us straight about pore pressures in faults and to David Foster for constructive criticism. This work would not have been possible without the help of the following people: Umberto Fuenzalida, Hernan Marilao, Carmen Gloria of the Universidad de Chile; Corporacion Nacional Forestal de Chile (CONAF)—Juan Fica, Claudio Manzur, Carlos Llautureo; Sra. Monica Retamal Maturana, Banco Estado; Carabineros de Chile del Region de Aysen; Armada de Chile; Cuerpo Militar de Trabajo del Ejercito de Chile (Cmdte. Roldan, Maj. Wellkner); Alcaldes de Aysen, Melinka (Luis Miranda Chiguay), Rio Ibanez, Lago Verde; Ejercito de Chile; Aeronautica de Chile (Sr. Carlos Feliu Ruiz); Automotriz Varona (Don Luis Hidalgo); Don Gustavo Lopez y Hostal Bon; Mike Fort, Noel Barstow, Bruce Beaudoin, Jim Fowler of IRIS PASSCAL; Tripulacion de LM Petrel IV (CONAF): Juan Gallardo, Axel Hernandez, Hernan Aguilar, Jose Geicha Nauto; Gilles Rigaud, Aurelia Rigaud, Valerie Clouard, Lorena Palacio et Morgane; Eduardo Moscoso, Javier; Don Raul Hernandez, Fundo Los Nirres; Ing. Sergio Mirando Contreras (Melinka); Escuela Carlos Condell, Calete Andrade, Pto. Aguirre (Sr. Victor Figueroa); Enrique Alcalde (Cochrane); Luis Levin (Bahia Murta); Baterias GAMI (Puerto Montt); Mauricio Zambrano L. (Coyhaique Centro de Llamadas); Rolando Burgos and Roselia Delgado, Fachinal; Aladin Jara, Gob. De Chile Chico; Rolando Toloza, Min. Obras Publicas; Mark and Sra. Knipreth, Heart of the Andes Lodge; Tripulacion de El Aleph: Heraldo Zapata Rivera, Ramon Villegas, Omar Tapia Vidal, Jorge Oyarzun Inostroza; Sandalio Munoz, Fundo La Pedregosa; Don Cristian Brautigam and the many, many people of Region XI, Aysen, who helped us enthusiastically and unstintingly and without whose help this work would have been much less fun. This work was funded by U.S. National Science Foundation grant No. 0126244 and CONICYT-CHILE grant No. 1050367. CM particularly acknowledges the Universidad de Chile for the scholarship 'Becas de Estadias Cortas de Investigación Destinadas a Estudiantes Tesistas de Doctorado y Magíster de la Universidad de Chile'.

REFERENCES

Arancibia, G., Cembrano, J. & Lavenu, A., 1999. Transpresión dextral y partición de la deformatión en la zone de Falla Liquiñe-Ofqui, Aisén, Chile, *Rev. Geol. Chile,* **26,** 3–22.

Beck, M.E., Rojas, C. & Cembrano, J., 1993. On the nature of buttressing in margin-parallel strike-fault systems, *Geology,* **21,** 755–758.

Cembrano, J., Beck, M.E., Burmester, R.F., Rojas, C., Garcia, A. & Herve, F., 1992. Paleomagnetism of Lower Cretaceous rocks from east of the Liquine-Ofqui fault zone, southern Chile: Evidence of small in-situ clockwise rotations, *Earth planet. Sci. Lett.,* **113,** 539–551.

Cembrano, J., Hervé, F. & Lavenu, A., 1996. The Liquine–Ofqui fault zone: a long-lived intra-arc fault system in southern Chile, *Tectonophysics,* **259,** 55–66.

Cembrano, J., Lavenu, A., Reynolds, P., Arancibia, G., Lopez, G. & Sanhueza, A., 2002. Late Cenozoic transpressional ductile deformation north of the Nazca-South America–Antarctica triple junction, *Tectonophysics,* **354,** 289–314.

Cifuentes, I.L., 1989. The 1960 Chilean earthquakes, *J. geophys. Res.,* **94,** 665–680.

Dewey, J.W., 1972. Seismicity and tectonics of western Venezuela, *Bull. seism. Soc. Am.,* **62,** 1711–1751.

Douglas, A., 1967. Joint epicentre determination, *Nature,* **215**, 47–48.

Ekstrom, G., Dziewonski, A. & Nettles, M., 2006. The Global CMT Project, www.globalcmt.org (last accessed 2009 July 30).

Freed, A.M., 2005. Earthquake triggering by static, dynamic and post-seismic stress transfer, *Ann. Rev. Earth planet. Sci.,* **33,** 335–367, doi:10.1146/annurev.earth.33.092203.122505.

Haberland, C., Rietbrock, A., Lange, D., Bataille, K. & Hofmann, S., 2006. Interaction between forearc and oceanic plate at the south-central Chilean margin as seen in local seismic data, *Geophys. Res. Lett.,* **33,** L06311, doi:10.1029/2006GL029190.

Harris, R.A., 1998. Introduction to special section: stress triggers, stress shadows, and implications for seismic hazard, *J. geophys. Res.,* **103,** 24 347–24 358.

Kennett, B.L.N., Engdahl, E.R. & Buland, R., 1995. Constraints on seismic velocities in the Earth from travel times, *Geophys. J. Int.,* **122,** 108–124.

King, G.C.P., Stein, R.S. & Lin, J., 1994. Static stress changes and the triggering of earthquakes, *Bull. seism. Soc. Am.,* **84,** 935–953.

Lange, D., Rietbrock, A., Haberland, C., Bataille, K., Dahm, T., Tilmann, F. & Flüh, E.R., 2007. Seismicity and geometry of the south Chilean subduction zone (41.5–43.5S): implications for controlling parameters, *Geophys. Res. Lett.,* **34,** L06311, doi:10.1029/2006GL029190.

Lange, D., Cembrano, J., Rietbrock, A., Haberland, C., Dahm, T. & Bataille, K., 2008. First seismic record for intra-arc strike-slip tectonics along the Liquine–Ofqui fault zone at the obliquely convergent plate margin of the southern Andes, *Tectonophysics,* **455,** 14–24.

Lin, J. & Stein, R.S., 2004. Stress triggereing in thrust and subduction earthquakes and stress interaction between the southern San Andreas and nearby thrust and strike-slip faults, *J. geophys. Res.,* **109,** B02303, doi:10.1029/2003JB002607.

Ma, K.-F., Chan, C.-H. & Stein, R.S., 2005. Response of seismicity of Coulomb stress triggers and shadows of the 1999 M (sub w) = 7.6 Chi-chi, Taiwan, earthquake, *J. geophys. Res.,* **110,** doi:10.1029/2004JB003389.

Marshall, J.L. & Russo, R.M., 2005. Relocated aftershocks of the March 10, 1988 Trinidad earthquake: normal faulting, slab detachment, and extension at upper mantle depths, *Tectonophysics,* **398,** 101–114.

Mora, C., Comte, D., Russo, R., Gallego, A. & Mocanu, V., 2010. Aysen seismic swarm (January 2007) in southern Chile: analysis using joint hypocentral determination, *J. Seismol.,* **14,** 683–691.

Murdie, R.E., Prior, D.J., Styles, P., Flint, S.S., Pearce, R.G. & Agar, S.M., 1993. Seismic repsonses to ridge-transform subduction: Chile triple junction, *Geology,* **21,** 1095–1096.

Pardo-Casas, F. & Molnar, P., 1987. Relative motion of the Nazca (Farallón) and South American Plates since Late Cretaceous time, *Tectonics,* **6,** 233–248.

Pollitz, F.F. & Sacks, I.S., 1992. Modeling of postseismic relaxation following the great 1857 earthquake, southern California, *Bull. seism. Soc. Am.,* **82,** 454–480.

Pollitz, F.F. & Sacks, I.S., 1997. The 1995 Kobe, Japan, earthquake: a long-delayed aftershock of the offshore 1944 Tonankai and 1946 Nankaido earthquakes, *Bull. seism. Soc. Am.,* **85,** 1–10.

Rojas, C., Beck, M.E., Burmester, R.F., Cembrano, J. & Hervé, F., 1994. Paleomagnetism of the Mid-Tertiary Ayacara Formation, southern Chile: counterclockwise rotation in a dextral shear zone, *J. South Am. Earth Sci.,* **7,** 45–56.

Rosenau, M., Melnick, D. & Echtler, H., 2006. Kinematic constraints on intra-arc shear and strain partitioning in the southern Andes between 38°S and 42°S latitude, *Tectonics,* **25,** TC4013, doi:10.1029/2005TC001943.

Russo, R.M., Okal, E.A. & Rowley, K.C., 1992. Historical seismicity of the southeastern Caribbean and tectonic implications, *Pure appl. Geophys.,* **139,** 87–120.

Schwartz, S.Y. & Rakosky, J.M., 2007. Slow slip events and seismic tremor at circum-Pacific subduction zones, *Rev. Geophys.,* **45,** doi:10.1146/annurev.earth.33.092203.122505.

Stein, R.S., 1999. The role of stress transfer in earthquake occurrence, *Nature,* **402,** 605–609.

Stein, R.S., 2003. Earthquake conversations, *Sci. Am.,* **288,** 72–79.

Stein, S.A. & Wysession, M.E., 2003. *An Introduction to Seismology, Earthquakes, and Earth Structure,* p. 498, Blackwell Publishing, Oxford, UK.

Toda, S. & Stein, R.S., 2003. Toggling of seismicity by the 1997 Kagoshima earthquake couplet: a demonstration of time-dependent stress transfer, *J. geophys. Res.,* **108,** doi:10.1029/2003JB002527.

Toda, S., Stein, R.S., Richards-Dinger, K. & Bozkurt, S., 2005. Forecasting the evolution of seismicity in southern California: animations built on earthquake stress transfer, *J. geophys. Res.,* **110,** B05S16, doi:10.1029/2004JB003415.

Wang, K., Hu, Y., Bevis, M., Kendrick, E., Vargas, R.B. & Lauria, E., 2007. Crustal motion in the zone of the 1960 Chile earthquake: detangling earthquake-cycle deformation and forearc-sliver translation, *Geochem. Geophys. Geosyst.,* **8,** Q10010, doi:10.1029/2007GC001721.

Wysession, M.E., Okal, E.A. & Miller, K.L., 1991. Intraplate seismicity of the Pacific Basin, 1913–1988, *Pure appl. Geophys.,* **135,** 261–359.